Supporting Information

Membrane Active Janus-Oligomers of β³-Peptides

Imola Cs. Szigyártó[a], Judith Mihály[a], András Wacha[a], Dóra Bogdán[a,b], Tünde Juhász[a], Gergely Kohut[a,c], Gitta Schlosser[c], Ferenc Zsila[a], Vlada Urlacher[d], Zoltán Varga[a], Ferenc Fülöp[e], Attila Bóta[a], István Mándity[a,b*], Tamás Beke-Somfai[a,f*]

[a] Institute of Materials and Environmental Chemistry, Research Centre for Natural Sciences, H-1117 Budapest, Hungary
[b] Department of Organic Chemistry, Faculty of Pharmacy, Semmelweis University, H-1092 Budapest, Hungary
[c] Institute of Chemistry, Eötvös Loránd University, H-1117 Budapest, Hungary
[d] Institute of Biochemistry, Heinrich-Heine University, 40225 Düsseldorf, Germany
[e] MTA-SZTE Stereochemistry Research Group, Institute of Pharmaceutical Chemistry, University of Szeged, H-6720 Szeged, Hungary
[f] Department of Chemistry and Chemical Engineering, Physical Chemistry, Chalmers University of Technology, SE-41296 Göteborg, Sweden

Table of Contents

1. Materials and Methods

General: High purity synthetic 1,2-dioleoyl-*sn*-glycero-3-phosphocholine (DOPC), 1,2-dioleoyl-*sn*-glycero-3-[phospho-*rac*-(1-glycerol)] (sodium salt) (DOPG) and 1,2-dipalmitoyl-*sn*-glycero-3-phosphocholine (DPPC), were purchased from the Avanti Polar Lipids Inc. (USA). All materials were used without further purification. Fmoc-protected amino acids were purchased from Sigma-Aldrich (Hungary). Analytical reagent grade chloroform (LabScan, Hungary), methanol (Reanal, Hungary), trifluoroacetic acid (Sigma, Hungary) and dimethylformamide (Reanal, Hungary) were used for preparing the spreading solutions. All other reagents (trifluoroacetic acid, hexafluoroisopropanol, dioxane, pyrene, 8-anilinonaphtalene-1- sulfonic acid (ANS), Thioflavin-T (ThT)) were purchased from Sigma-Aldrich (Hungary). Coupling reagents and additives, including *N,N*-dimethylforamide, dichloromethane, methanol, acetonitrile, acetic acid were purchased from Macron Fine Chemicals; 1,8-diazabicyclo[5.4.0]undec-7-ene (DBU), piperidine, 1-[*bis* (dimethylamino)-methylene]-1*H*-1,2,3-triazolo[4,5-b]pyridinium-3-oxide (HATU), *N,N*-diisopropylethylamine (DIPEA). The TentaGel R RAM resin was purchased from Rapp Polymere GmbH.

Peptide synthesis

All peptides were synthesized by a solid-phase technique, utilizing Fmoc chemistry. The peptide chains were elongated on a TentaGel R RAM resin (0.19 mmol/g). The couplings were performed with 2 equivalents of Fmoc-protected amino acid and 2 equivalents of HATU and 4 equivalents of DIPEA were used in 1.5 mL N,N-dimethylformamide (DMF) as solvent. The coupling reactions were carried out at the optimized reaction conditions, 60 bar, 70 °C, 0.15 mL/min flow rate. For Fmoc deprotection 2 mL of 2% DBU, 2% piperidine in DMF solution was used. The peptide sequences were detached from the resin with 90% TFA + 5% water + 2.5% triisopropylsilane + 2.5% dithiothreitol at room temperature for 3 h. The TFA was then removed and the resulting peptides were precipitated with cooled dried diethyl ether. The precipitated free peptides were filtered off, and then solubilized in 10% aqueous acetic acid and lyophilized.

Preparation of large unilamellar lipid vesicles

Liposomes were prepared by using the lipid thin film hydration technique. DOPC and DOPC/DOPG lipid mixture (molar ratio 90/10) with/without peptides were dissolved in chloroform containing 50 vol% methanol, except for peptide **1**, where polar solvent was hexafluoroisopropanol, which was then evaporated. The resulting lipid film was kept under vacuum for 8 hours to remove the residual trace amounts of solvent. The dried lipid film was hydrated with PBS buffer (pH 7.4). To achieve homogenous mixture, repeated heating (37°C) and cooling (-196°C) steps were applied. The solutions were extruded through polycarbonate filters with 100 nm pore size (at least 10 times) by using a LIPEX extruder (Northem Lipids Inc., Canada).

HPLC-Mass Spectrometry (HPLC-MS)

β-peptides purity were determined by reverse-phase HPLC on C18 Phenomenex Luna 5 μm column (4.6 mm× 250 mm), using gradient mobile phase (solvent A: consisted of 0.1% AcOH in water, and solvent B: 0.1% AcOH in 80% acetonitrile); the gradient was 5% – 50% B during 25 min or 5% – 80% B during 25 min, at a flow rate of 1 mL min^{-1}. The analysis was performed on a Dionex HPLC equipped with a Thermo LCQ Fleet mass spectrometer.

Attenuated total reflection Fourier-transform infrared spectroscopy (ATR-FTIR)

FTIR spectra were collected using a Varian 2000 spectrometer (Scimitar Series, Varian Inc, USA) equipped with a liquid nitrogen cooled mercury-cadmium-telluride (MCT) detector and with a 'Golden Gate' single reflection diamond ATR accessory (Specac Ltd, UK). Approximately 5 μL of sample was pipetted onto the diamond ATR surface and a thin dry film was obtained after slowly evaporation of the solvent under ambient conditions. Typically, 64 scans were collected at a nominal resolution of 2 cm^{-1}. ATR correction and spectral manipulations including spectral subtraction, smoothing and Fourier self-deconvolution of the amide I band were performed using the GRAMS/32 software package (Galactic Industries Inc, USA).

NMR

NMR measurements of water soluble peptides **3-5** (4 mM in H_2O:D_2O 90:10) were carried out on a Bruker Avance III 500 MHz spectrometer equipped with a cryo probe head. ROESY

and TOCSY spectra were recorded for peptide **5** only and for ROESY spinlock, a mixing time of 300 ms was used. The number of scans was 16 and roesyesgpph pulse sequence was applied. The TOCSY measurement was performed with the mlevesgpph sequence, with a mixing time of 120 ms and the number of scans was 16. For all 2D spectra, 4k time domain points and 512 increments were applied. DOSY spectra of **3**-**5** were performed by the 2D LED experiment using bipolar gradients (ledbpgp2s). A time of 1.2 ms was used for the dephasing/refocusing gradient pulse length (δ) and 150 ms for the diffusion delay (Δ). The gradient strength was changed quadratically from 2 % to 98 % of the maximum value and the number of steps was 16. The measurement was run with 16 scans and 32k time domain points, using 1,4-dioxane as internal standard, with a hydrodynamic radius of 1.87Å[1]. The processing was carried out by using a cosine-bell window function, single zero filling and automatic baseline correction. The hydrodynamic radius was determined by the relationship of $R_h^{peptide} = (D_{dioxane}/D_{peptide}) \times R_h^{dioxane}$. Molar mass of the aggregate was calculated based on the relationship of $M_{peptide} = (D_{HOD}/D_{peptide})^3 \times M_{HOD}$ [2].

Circular dichroism spectroscopy (CD)

CD spectra were recorded on a Jasco J-715 spectropolarimeter in a 0.1 cm path length rectangular quartz cuvette (Hellma, USA) at room temperature. Peptides CD data were collected between 185 and 260 nm at a scan rate of 50 nm/min, with data pitch of 0.1 nm, and 3 times accumulations. CD curves were corrected by the spectral contribution of the blank aqueous solution.

Transmission electron microscopy (TEM)

For direct visualization of the structure and morphology of the samples transmission electron microscopy images were obtained on Morgagni 268D (FEI, The Netherlands). Approximately, 2 µl droplet of sample in aqueous solution was pipetted onto a 200 mesh copper grid and after 20 s contact time the excess of liquid was removed.

Dynamic light scattering (DLS)

Mean hydrodynamic diameter (D_h) and size distribution of the samples were measured using W130i dynamic light scattering apparatus (DLS, AvidNano, UK). Low volume disposable cuvettes with 1 cm path-length were used (UVette, Eppendorf Austria GmbH). The analysis of the measurement data was performed with the i-Size software, supplied with the device.

Differential scanning calorimetry (DSC)

Calorimetric measurements were investigated using a Setaram μDSC3 EVO (Setaram, France) apparatus. Peptides **3-5** were mixed with DPPC lipid (1 to 10 molar ratio and a final total lipid concentration of 68 mM) and were dissolved in chloroform containing 50 vol% methanol, which was then evaporated. The resulting lipid film was kept under vacuum for 8 hours to remove the residual trace amounts of solvent. The dried lipid film was hydrated with PBS buffer (pH 7.4). To achieve homogenous mixture, repeated heating (37°C) and cooling (-196°C) steps were applied. Approximately 20 mg samples were loaded per measurements and an empty sample holder was used as a reference. The heating protocol consisted of 3 cycles from 20 to 50 °C. The scan rates were initially 1 °C/min, and 0.2 °C/min during the heating period, as well as 1 °C/min during the cooling period.

Fluorescence spectroscopy

Spectra were collected using a Jobin Yvon Fluoromax-3 spectrofluorimeter at 25°C in PBS, using a quartz micro cuvette of 3x3 mm path length. The ANS and ThT probe molecules were excited at 388 and 450 nm, and emission were monitored from 400 to 600 nm and 460 to 600 nm, respectively. Titration experiments were performed using 5 μM ANS and 25 μM ThT with increasing amounts of peptides **3-5** up to 250 μM. For comparison, ANS fluorescence was also measured with PC liposomes at 100 μM lipid concentration. Spectra were corrected for light scattering by subtracting the matching blank (peptide solutions at the same concentration). Data presented here are mean ± standard error of mean (SEM), (n=2-4).

Molecular dynamics simulations (MD)

In order to study the oligomerization process and structural properties of the resulting assemblies, MD simulations were done according to the following procedure. First the peptide molecules (**3-5**) were prepared in fully extended conformation using a PyMOL plug-in developed recently by us for the molecular modeling of β-peptides [3]. The CHARMM36m additive biomolecular force field has been used with our recently published extension for β-amino acids A topology was constructed for the peptide using the "pdb2gmx" utility of GROMACS (version 2019.2). The peptide was placed in the center of a cubic box, where the lowest distance of the peptide from the walls was 0.3 nm. Residual strain in the molecule was removed by a short energy minimization using the steepest descent algorithm. The resulting simulation box was stacked in a 2×2×2 alignment using the "genconf" subprogram with

random rotations of each chain. The system of eight chains was solvated using a pre-equilibrated box of CHARMM-modified TIP3P water. Na^+ and Cl^- ions were added in approx. 150 mM concentration, ensuring a zero net charge of the whole system. Restraining the positions of the heavy atoms of the peptide molecules with 1000 kJ/mol/nm harmonic potentials, a steepest descent energy minimization run was carried out on the solvent to ensure hydration of the peptides and to remove voids and steric clashes. Temperature coupling was turned on during a 1ns MD run using the velocity rescaling thermostat [4] set to 300 K with 0.1 ps characteristic time. In order to avoid the "hot solvent, cold solute" problem, two separate thermostats were used for the peptide and the solvent, respectively. After the temperature was stabilized, an isotropic Berendsen barostat [5] set to 1 bar was switched on using 5 ps coupling time. The isothermal compressibility of water ($4.5*10^{-5}$ bar^{-1}) was used. To ensure that the correct statistical ensemble is sampled, production runs were carried out using a Nosé-Hoover thermostat [6,7] with 0.8 ps coupling time and an isotropic Parrinello-Rahman barostat [8,9] with 5 ps coupling time. For all MD simulations, 2 fs time step size was used. Similar setting parameters were used for simulations in methanol solvent.

Membrane simulations were carried out using the same software and modified force field as applied for peptide **3-5**. A solvated DOPC bilayer of 128^x128 lipids was created using the CHARMM-GUI [10]. The two layers of the octameric bundles of peptide **5** resulted from simulations in aqueous solution were first turned inside out (compared to their equilibrium structure in water) to ensure compatibility with the hydrophobic environment. The bundles were then moved into the lipid bilayer and the spatial overlaps between the peptide **5** bundle atoms and DOPC lipid atoms were found and removed. Chimera 1.13.1 [11] was used for moving the bundles into DOPC bilayer and finding the DOPC atoms with spatial overlaps, while a python script was applied to remove them from the structure file. After the initial preparation, the systems were minimized and equilibrated as described in the following step: first the energy minimization was done using the steepest decent method in 5000 steps (emstep = 0.01 nm) with a maximum force tolerance of 1000 kJ mol^{-1} nm^{-1}, followed by 50 ps and 100 ps NVT equilibration using Berendsen thermostat for temperature coupling with a time constant of τT=1.0 ps. In the following steps 100 ps, 200 ps, 200 ps and 50ns NPT equilibration using Berendesen thermostat for temperature coupling with a time constant of τT=1.0 ps and semiisotropic Berendsen barostat in x-y and z direction for pressure coupling with a time constant of τP=5.0 ps were used with compressibility of $4.5*10^{-5}$ and 1 bar pressure, respectively. 1000 ns production runs were done using Nosé-Hoover thermostat and

Parrinello-Rahman barostat to ensure correct statistical ensembles, using the same parameters as for equilibration. Separate thermostats were used for peptide, DOPC bilayer and waters and ions both in equlibration and production run. The monomeric form of peptide **5** as well as tetrameric and octameric bundles of this peptide were moved into the middle of lipid bilayer. The positions of the bundles are defined as the distance between the z coordinate of their COM (center of mass) and the COM of the DOPC bilayer, whereas surfaces positions are defined as the distance between the z coordinate of the COM of phosphorous atoms or carbonyl groups of the acyl chains and the COM of the bilayer.

The initial state for MD studies of pyrene insertion into oligomeric bundles of peptide **5** was the frame from the trajectory of the octameric assembly with the largest number of hydrogen bonds. The β-peptide oligomer has been re-solvated in CHARMM-modified TIP3P water without changing the original box size. The force field parameters for pyrene have been obtained using the CGenFF generalized force field extension for CHARMM [12,13] using the ParamChem interface (CGenFF program version 2.2.0, for use with CGenFF version 4.0). A single pyrene molecule was inserted into the box containing the solvated β-peptide aggregate using the "insert-molecule" tool of GROMACS. The same equilibration steps were performed as for the previous simulation, including energy minimization of the solvent and turning on the thermostat and barostat. Finally, 1 μs sampling run was performed. Association/insertion of the pyrene molecule to the oligomeric bundles can be followed through measuring pair distances. Four characteristic atom groups were defined in the oligomer: the heavy (i.e. non-hydrogen) atoms of the N-terminal butyryl groups ("Nterm"), the last Leu residues ("Cterml"), the $–COO^-$ groups and the -N of the glutamate and lysine side-chains, respectively ("Hydrophilic") and the three outermost carbon atoms of all leucine side-chains in the third to fifth amino acid residues in the sequence ("HydrophobicCore"). The minimum distance of the center of gravity of the pyrene molecule from each of these atom groups has been measured in each frame of the trajectory.

2. HPLC- mass spectrometry

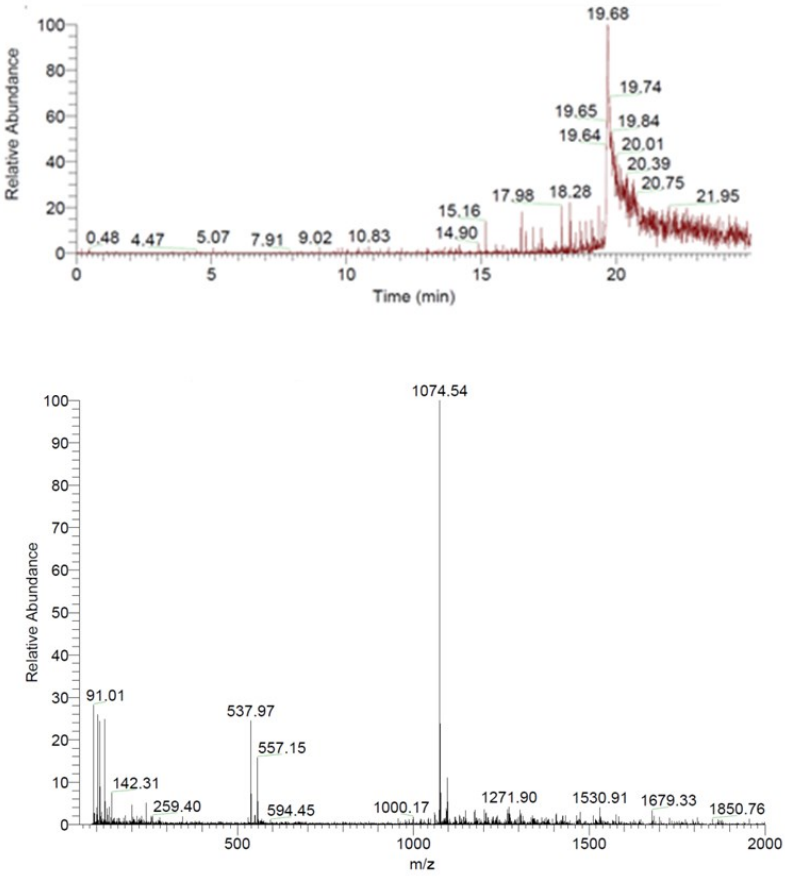

Figure S1. HPLC-MS chromatogram and mass spectrum of peptide **1**. *m/*z calculated for $[C_{60}H_{83}N_9O_9]$ ($[M+H]^+$) = 1074.63, observed ($[M+H]^+$) = 1074.54

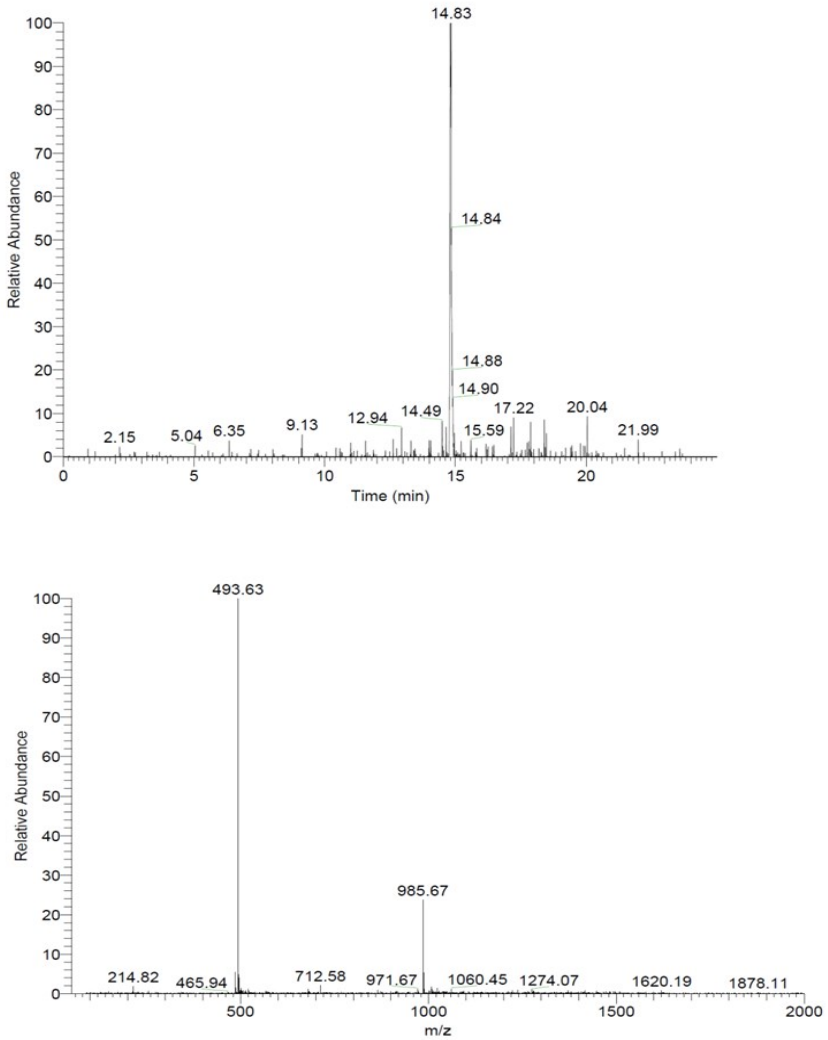

Figure S2. HPLC-MS chromatogram and mass spectrum of peptide **2**. *m/*z calculated for $[C_{51}H_{88}N_{10}O_9]$ ($[M+H]^+$) = 985.48, observed ($[M+H]^+$) = 985.67

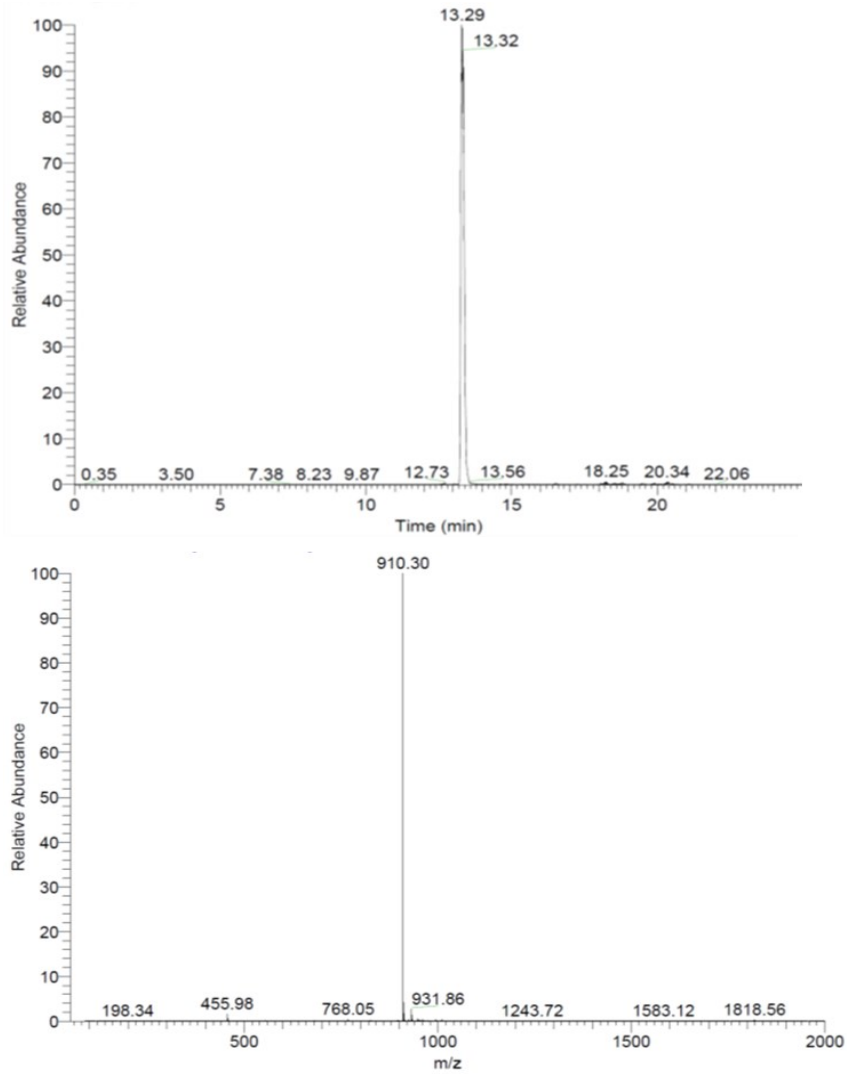

Figure S3. HPLC-MS chromatogram and mass spectrum of peptide **3**. *m/*z calculated for $[C_{45}H_{84}N_{10}O_9]$ ($[M+H]^+$) = 910.38, observed ($[M+H]^+$) = 910.30

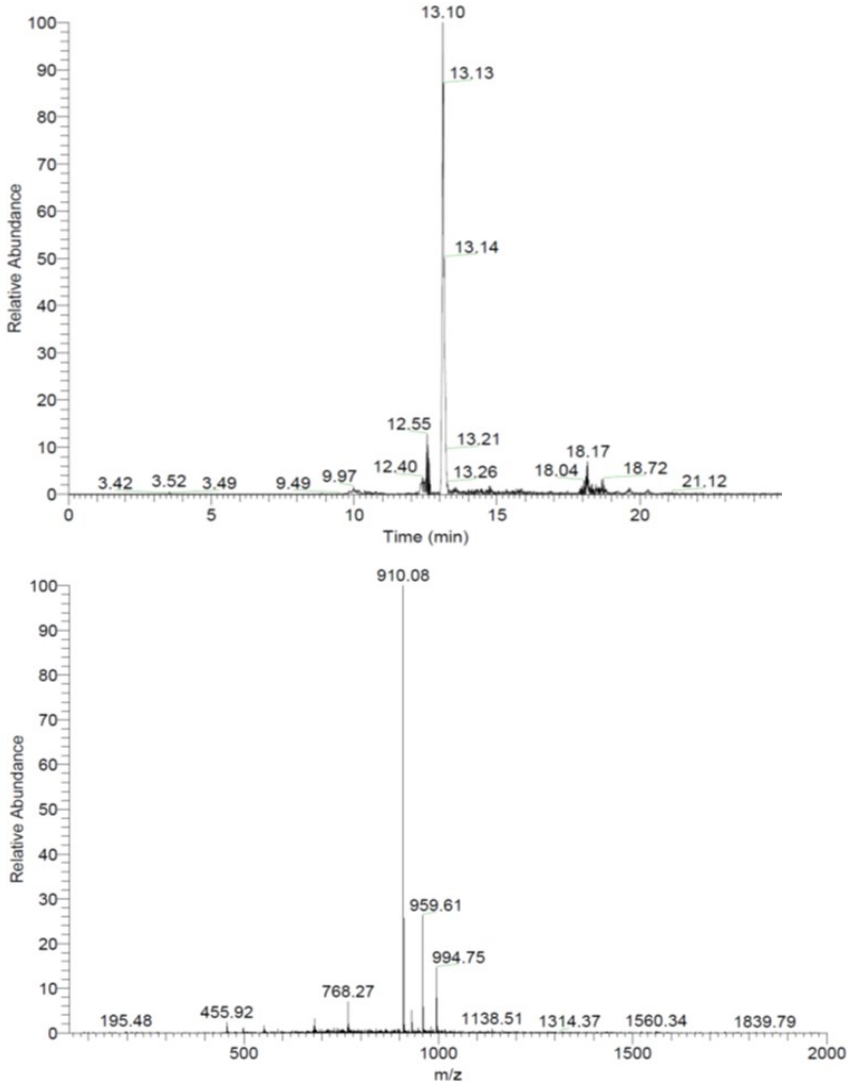

Figure S4. HPLC-MS chromatogram and mass spectrum of peptide **4**. *m/*z calculated for $[C_{45}H_{84}N_{10}O_9]$ ($[M+H]^+$) = 910.38, observed ($[M+H]^+$) = 910.06

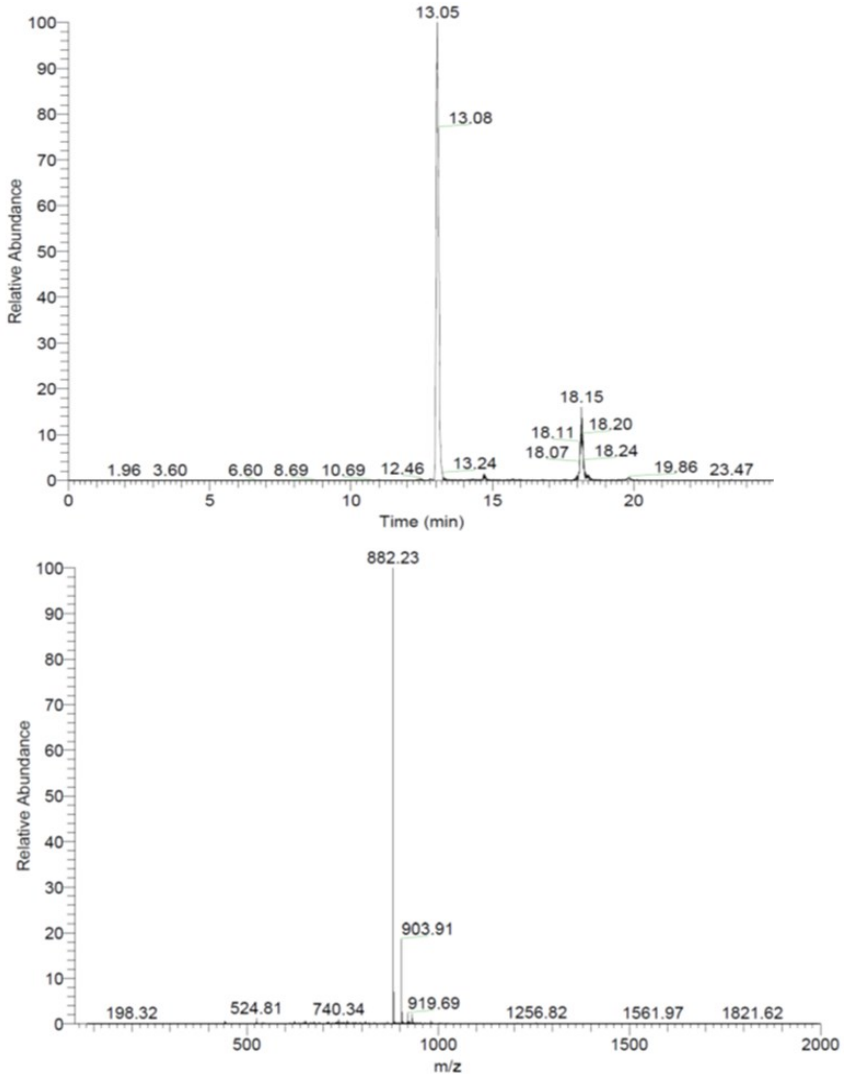

Figure S5. HPLC-MS chromatogram and mass spectrum of peptide **5**. *m/*z calculated for $[C_{45}H_{84}N_8O_9]$ ($[M+H]^+$) = 882.36, observed ($[M+H]^+$) = 882.23

3. Attenuated total reflection Fourier-transform infrared spectroscopy

Structure	**Peptides Amide I**				
	1 HFIP	**2** 10% AcOH	**3** H_2O	**4** H_2O	**5** H_2O
random coil	1648 (s)	1648 (s)	1646 (s)	1646 (s)	1646 (s)
sheet-like		1624, 1663 (w)	1630 (w)	1628, 1688 (w)	1690 (w)
weak H-bond			1658 (m)	1658 (m)	1658 (m)
Amide II					
	1541 (vw)	1551 (vw)	1546 (w)	1544 (w)	1546 (w)
		1536 (vw)		1534, 1560 (w)	1556, 1534

Table S1. Estimation of the characteristic components for peptide secondary structure. The complex amide I band of peptides (**1**-**5**) is decomposed by Fourier self-deconvolution method using Happ-Genzel apodization

function (bandwith 50 and enhancement 3). (For clarity the abbreviations for band intensity are: s = strong; m = medium; w = weak and vw = very weak).

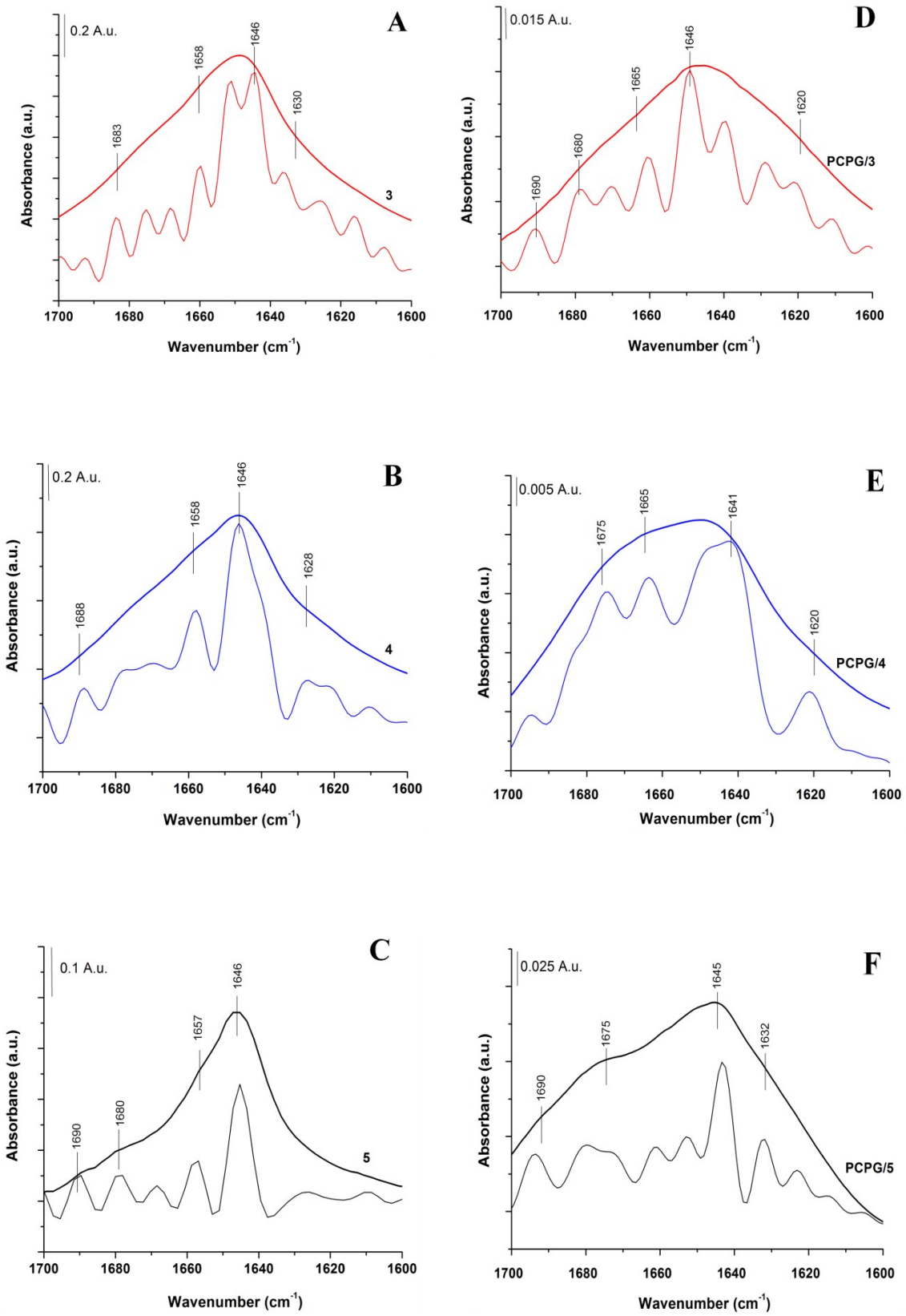

Figure S6. Deconvoluted amide I band of peptides **3** (A), **4** (B), **5** (C) in water and in the presence of unilamellar liposomes (**PCPG/3** (D), **PCPG/4** (E), **PCPG/5** (F)).

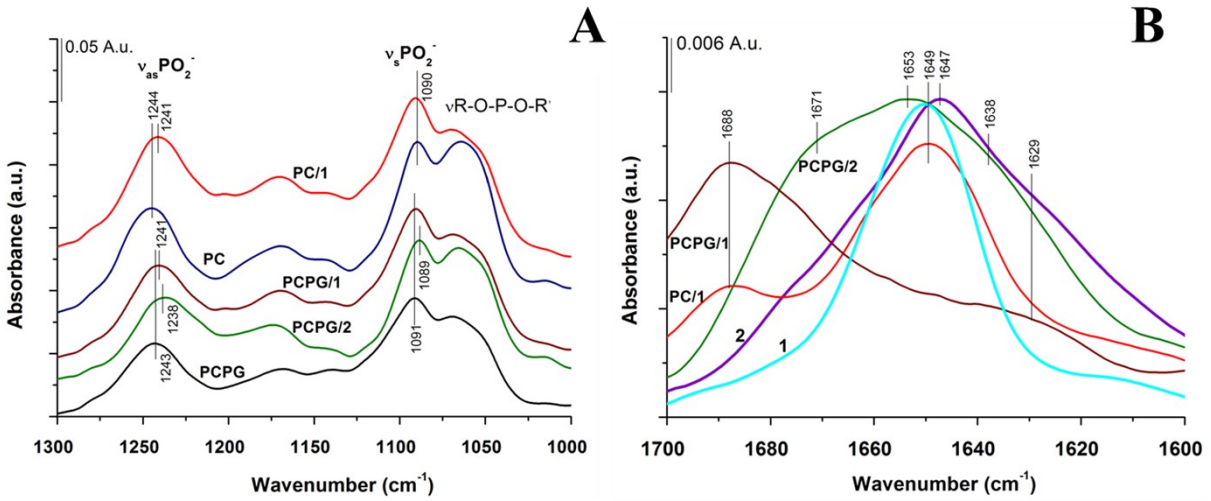

Figure S7. Infrared spectra of the foldamers **1** and **2**. A.) Phosphate and B.) Amide I regions of FTIR spectra recorded for liposome systems containing peptides **1** and **2** (PC = unilamellar DOPC and PCPG = unilamellar DOPC/DOPG liposomes). Spectra were recorded for dry films derived from solutions containing PC or PC/PG liposome (1.3 mM lipid) and peptides **1** and **2** (0.13 mM).

4. Nuclear magnetic resonance spectroscopy

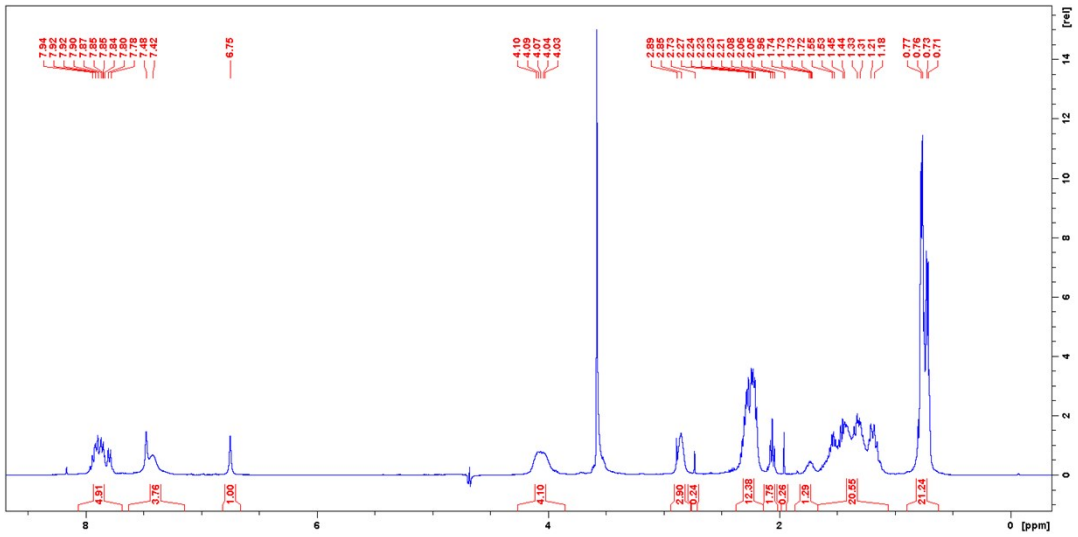

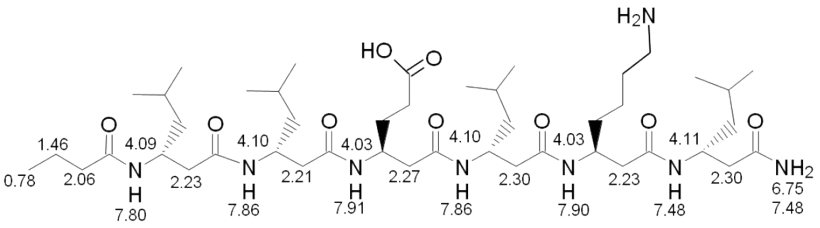

Figure S8. [1]H NMR spectrum of peptide **5** and assignment of backbone protons

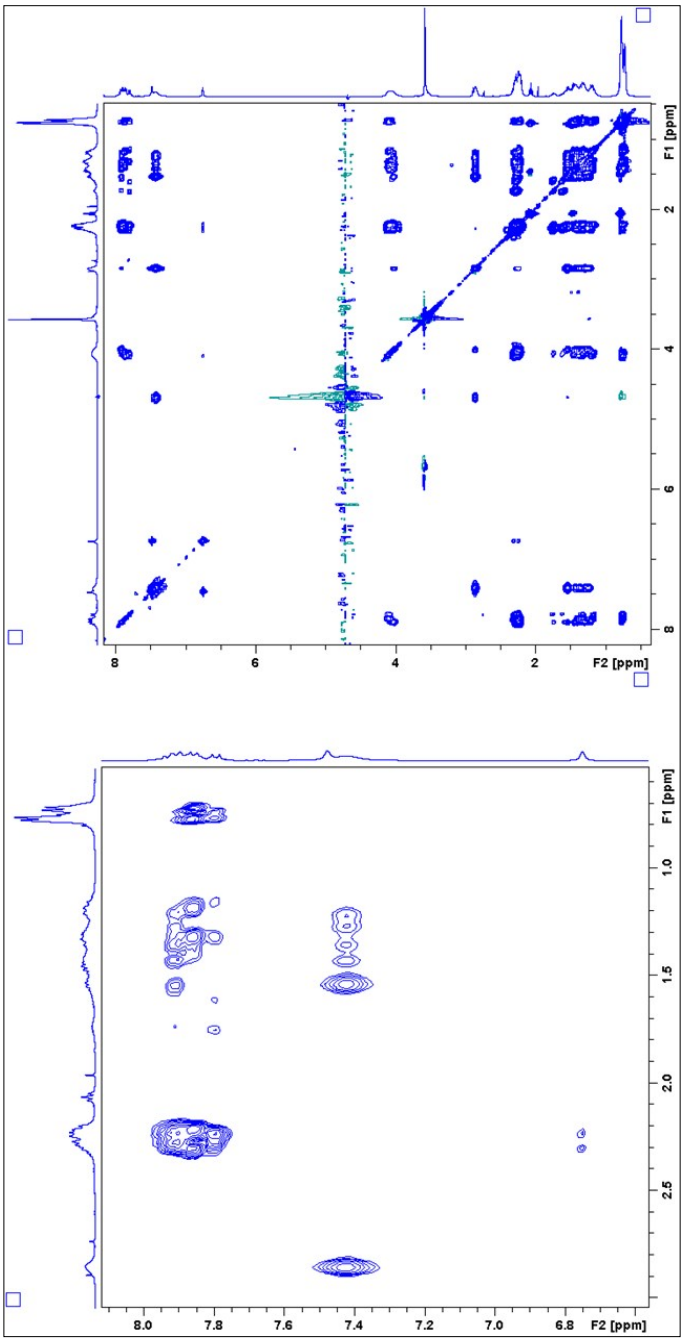

Figure S9. TOCSY-NMR spectrum of peptide **5**

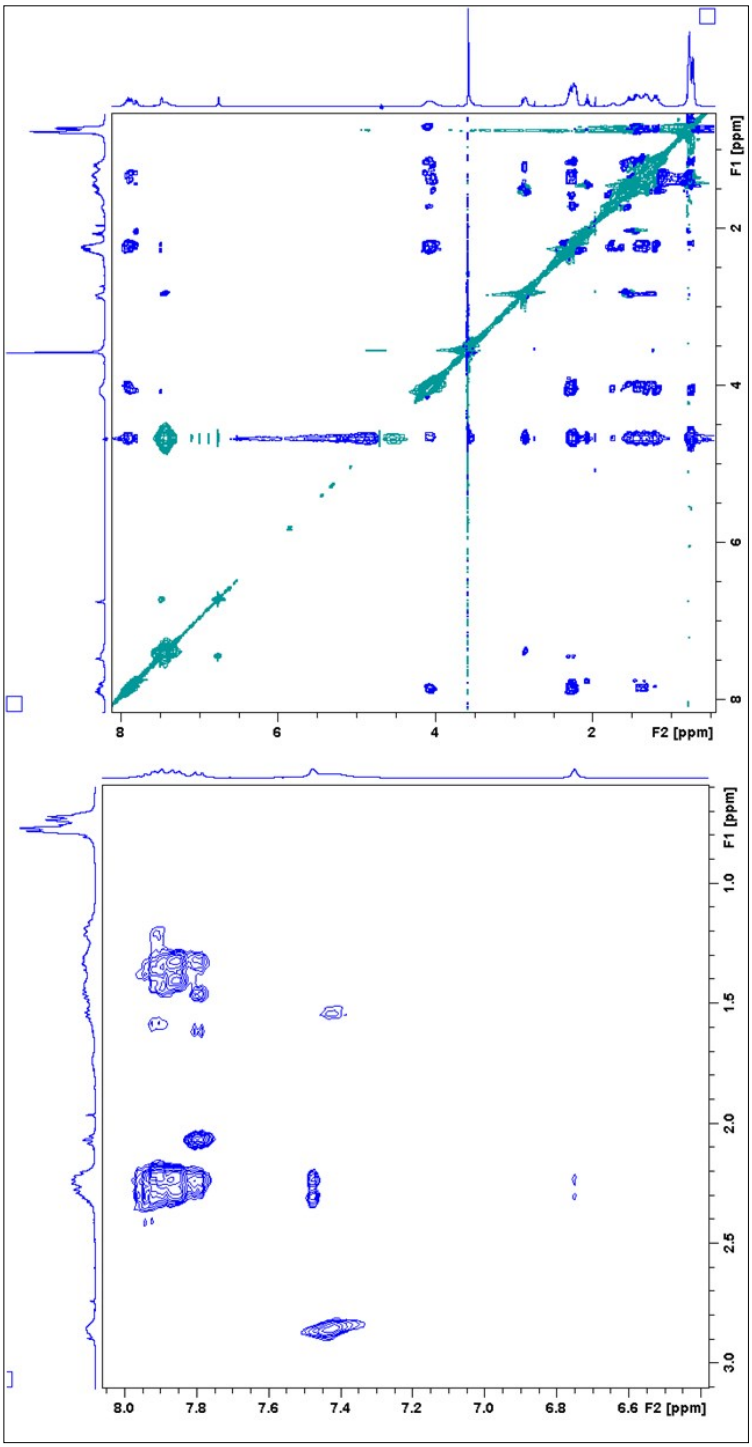

Figure S10. ROESY-NMR spectrum of peptide **5**

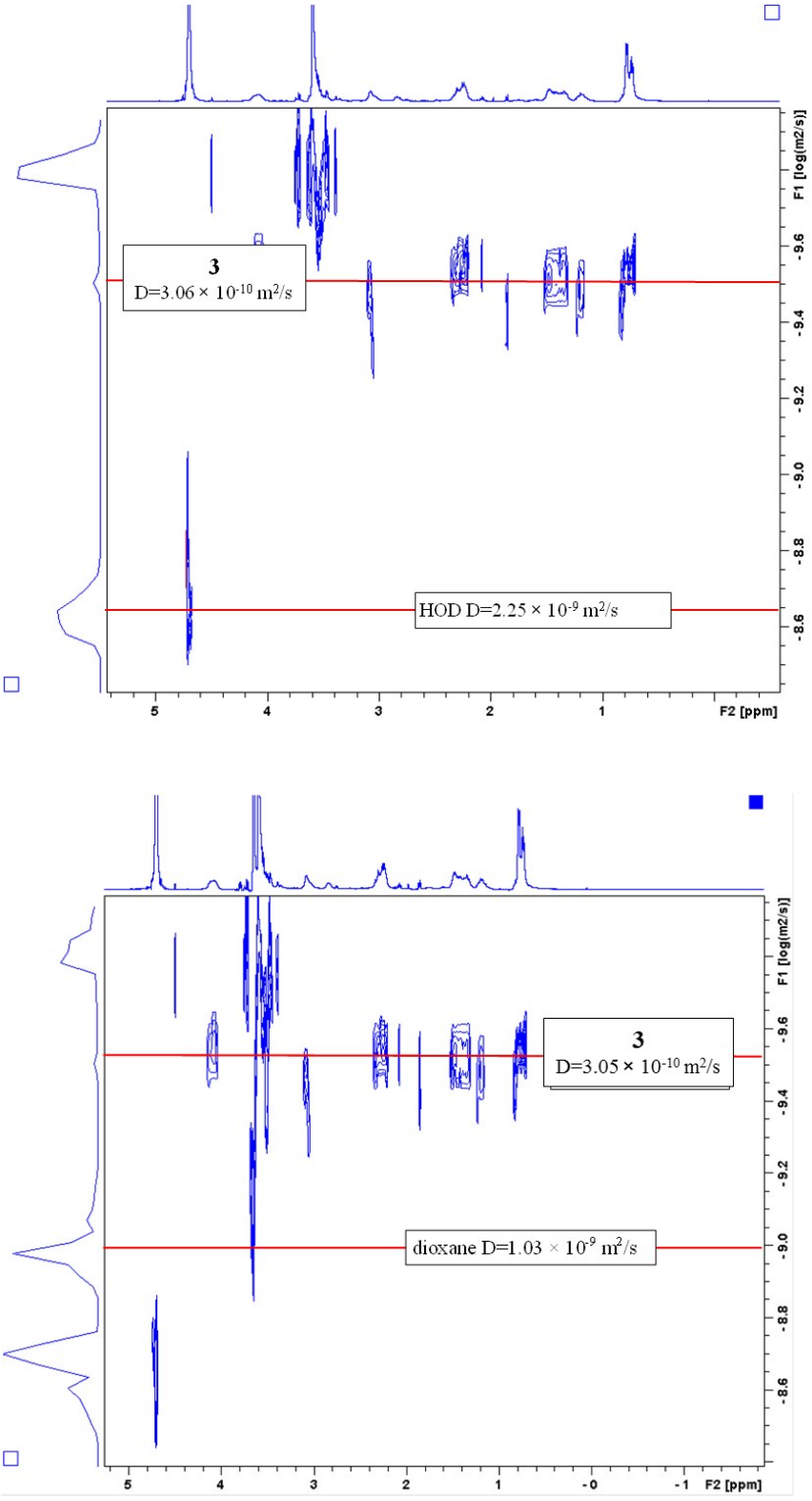

Figure S11. DOSY-NMR spectrum of peptide **3** in D_2O (top) and D_2O with dioxane (bottom)

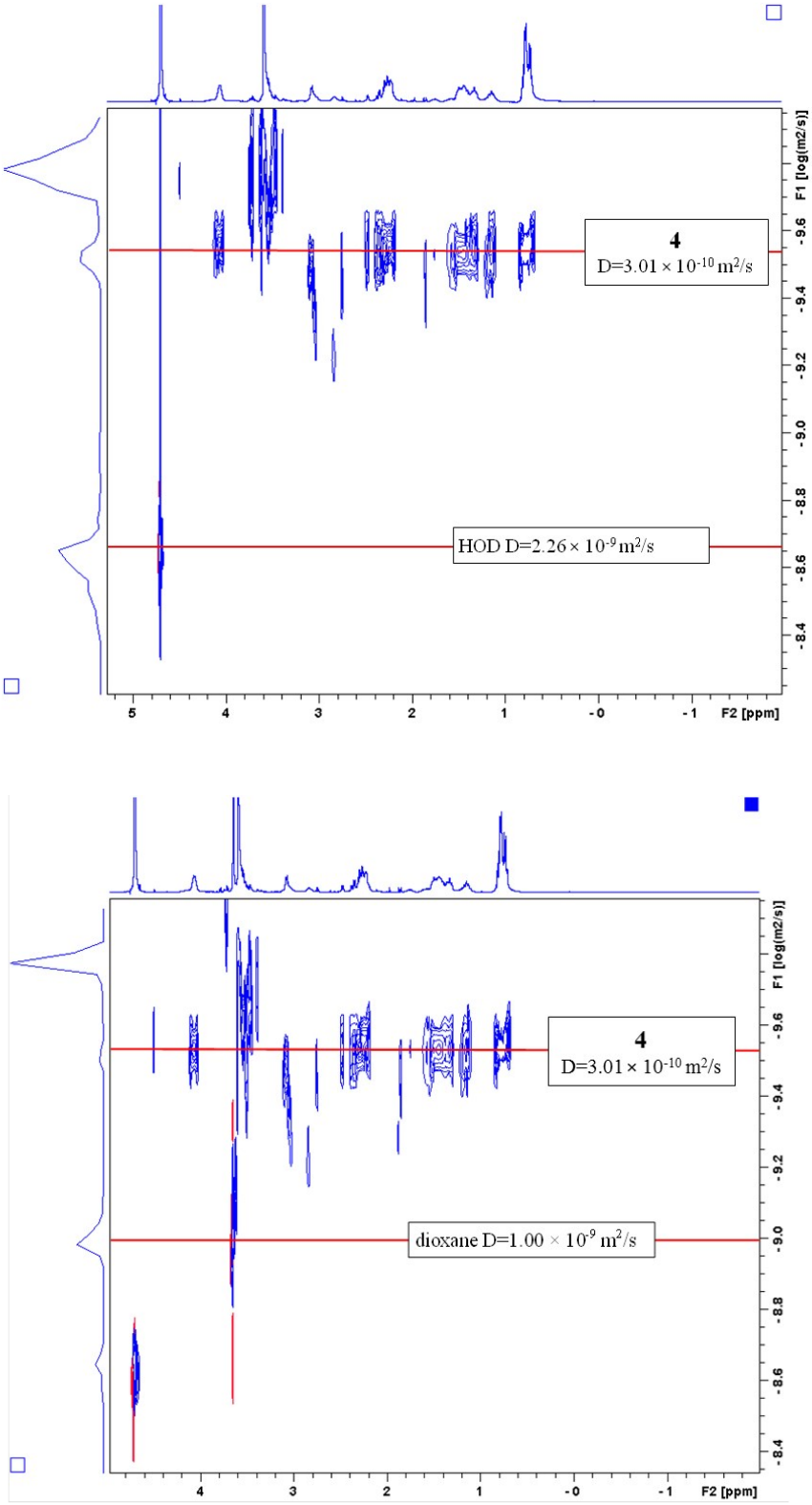

Figure S12. DOSY-NMR spectrum of peptide **4** in D_2O (top) and D_2O with dioxane (bottom)

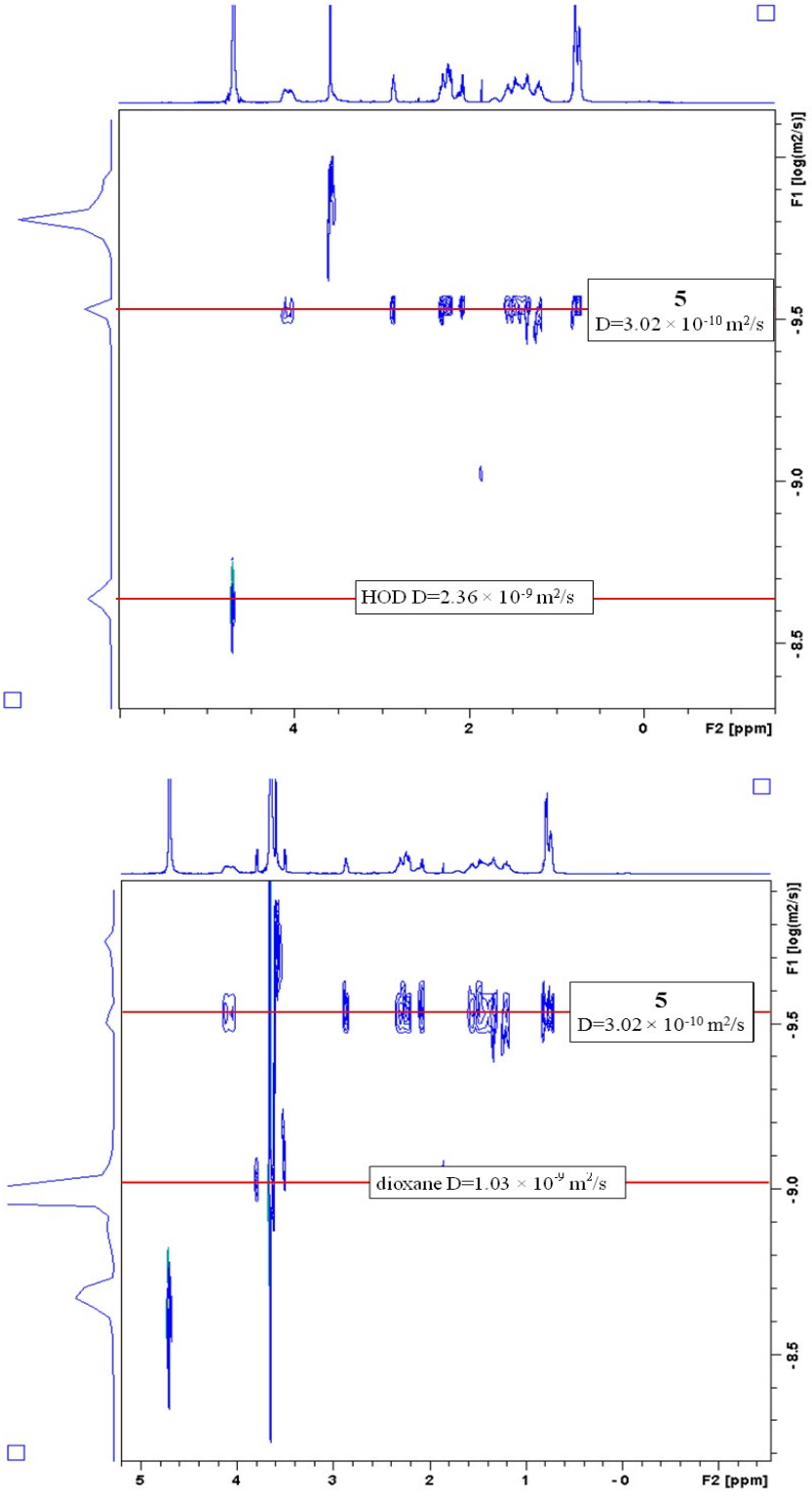

Figure S13. DOSY-NMR spectrum of peptide **5** in D_2O (top) and D_2O with dioxane (bottom)

5. Dynamic light scattering

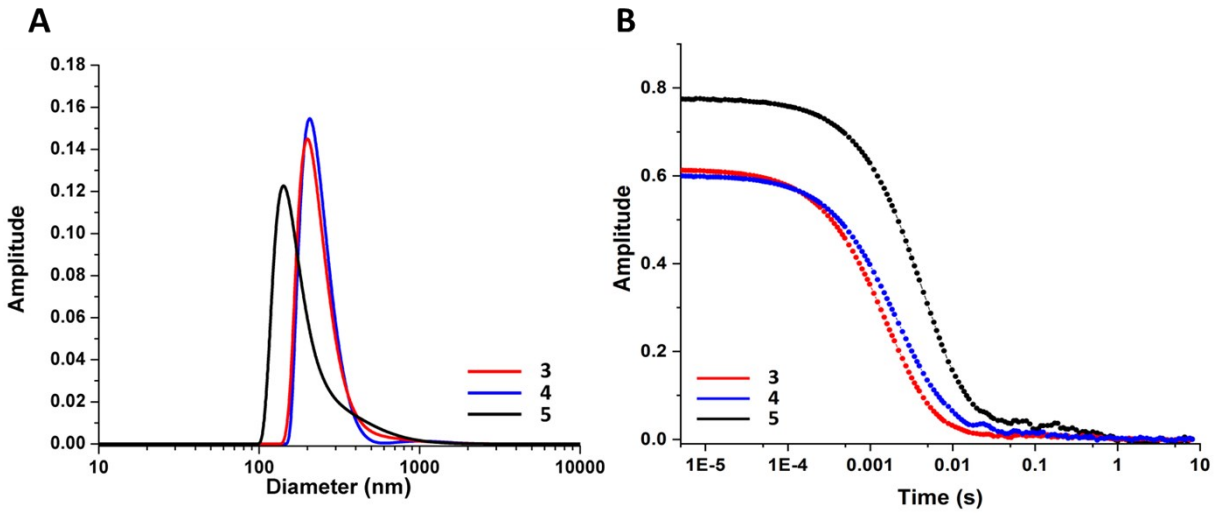

Figure S14. DLS size distribution (A) and correlation functions (B) of water soluble peptides (**3** – **5**) in water. Concentration used was 220 μM for each peptides.

6. Molecular dynamics simulations

The metric for classifying clusters was the RMS distance of the backbone atoms of residues 2-5, using a cut-off of 0.1 nm. Altogether 29 different folds were identified, the six most populated ones accounting for 95% of the whole trajectory.

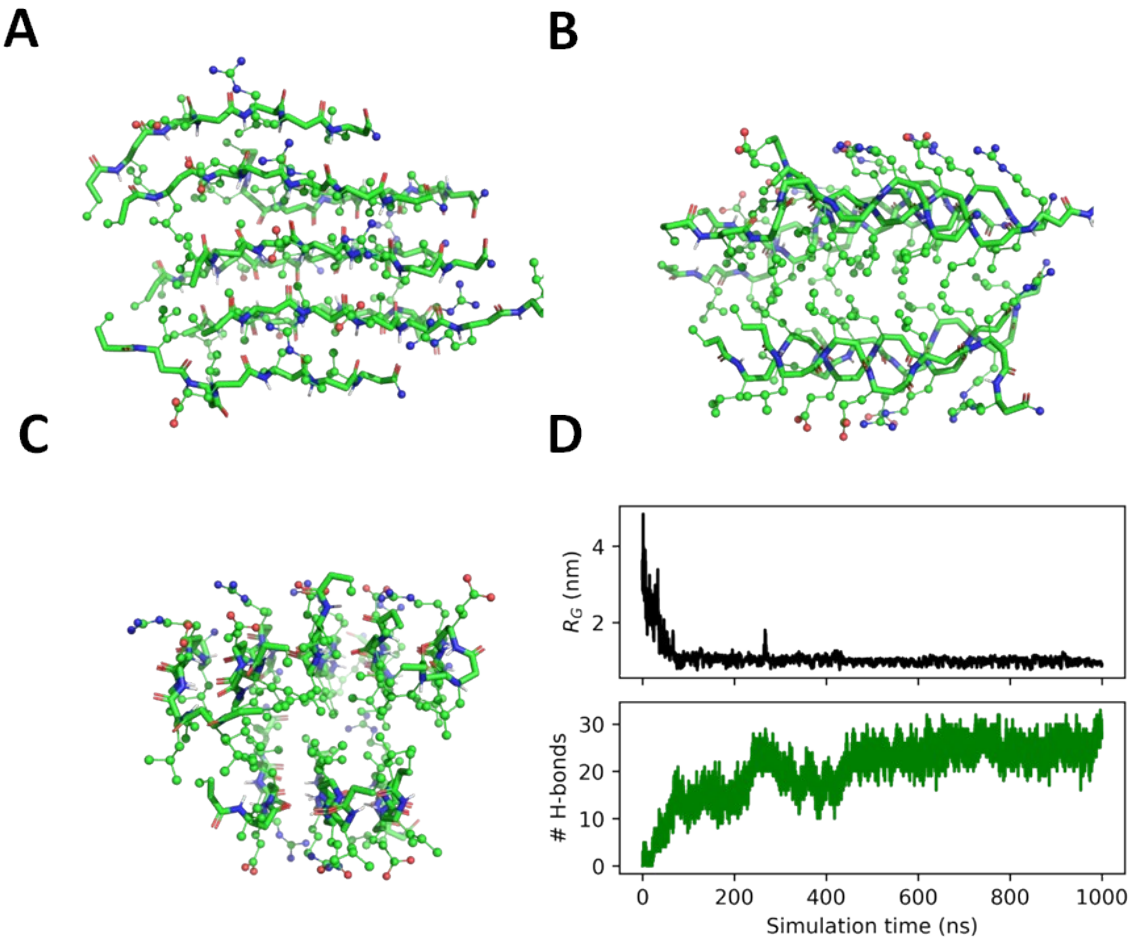

Figure S15. Self-assembly of peptides **3** into oligomeric bundles in water using 1 μs long MD simulations. A.) top view; B.) front view; C.) side view of the two-layered oligomer (layer one and two named as I. and II., respectively. (Color code: carbon, *green*, nitrogen, *blue*, oxygen, *red*) D.) Time-evolution of the gyration radius and the number of interchain hydrogen bonds during formation of octameric oligomer.

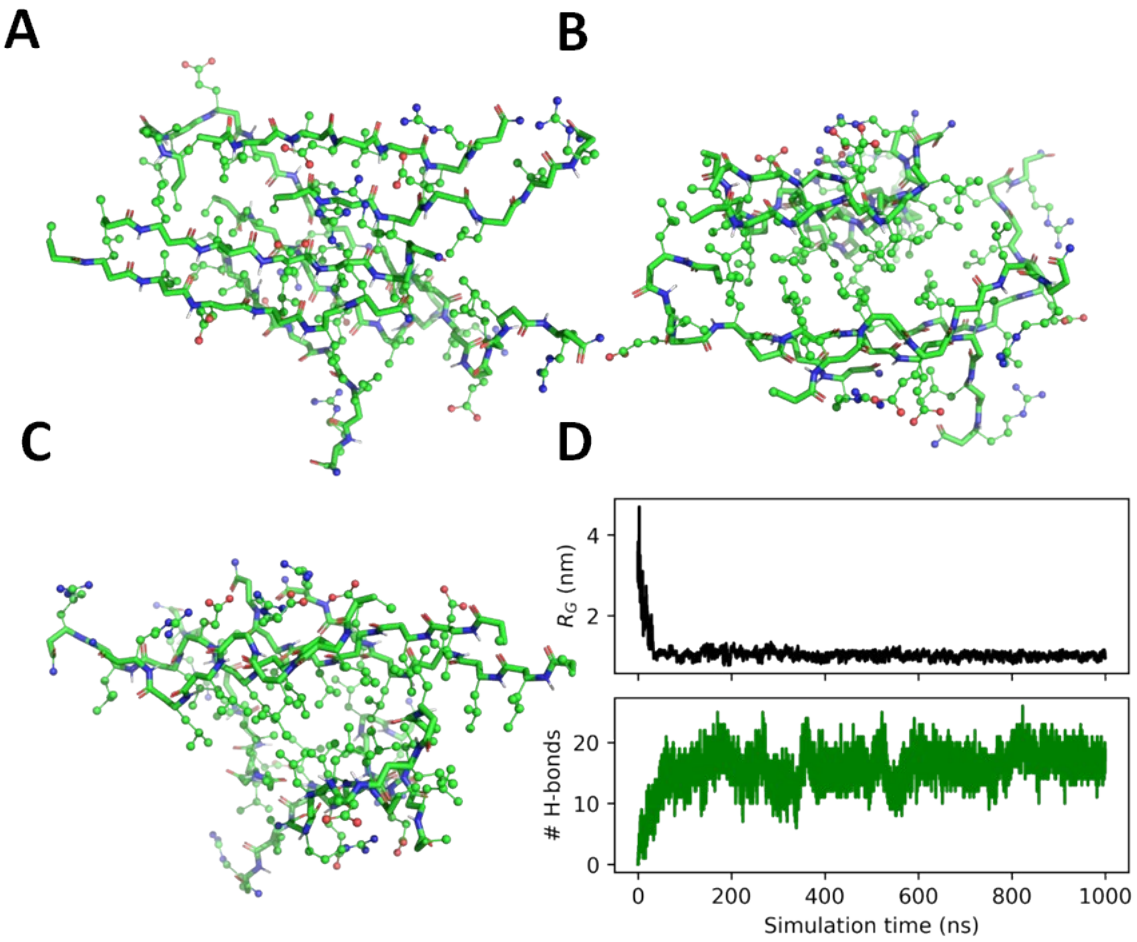

Figure S16. Self-assembly of peptides **4** into oligomeric bundles in water using 1 μs long MD simulations. A.) top view; B.) front view; C.) side view of the two-layered oligomer (layer one and two named as I. and II., respectively. (Color code: carbon, *green*, nitrogen, *blue*, oxygen, *red*) D.) Time-evolution of the gyration radius and the number of interchain hydrogen bonds during formation of octameric oligomer.

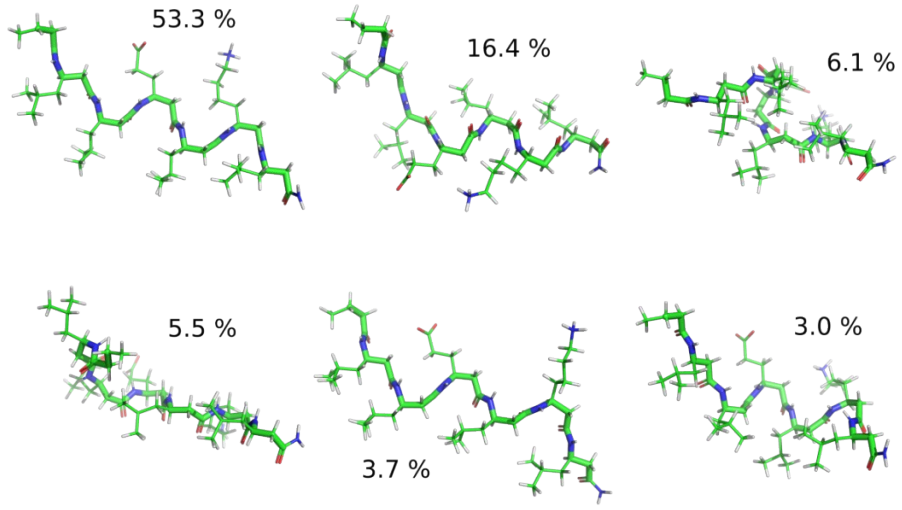

Figure S17. Representative elements of the four most populated backbone conformational states of peptide **5**

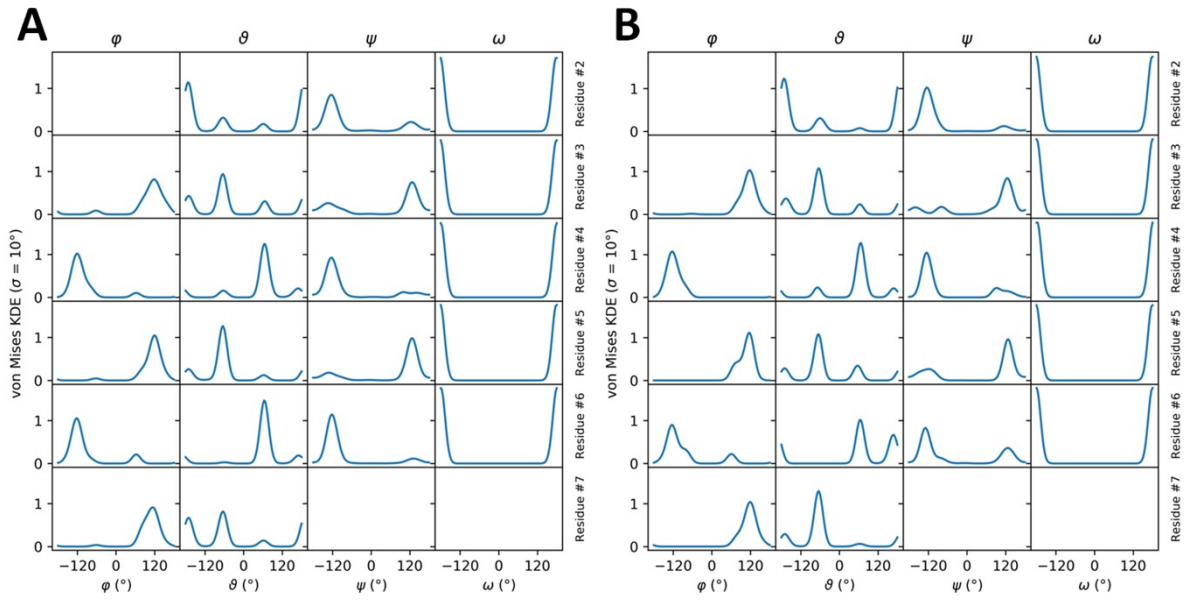

Figure S18. Kernel density estimates of the backbone torsional angles of the peptide **5** molecules in the aggregates in presence of: A.) in water, B.) in lipid bilayer. A periodic von Mises kernel was used with $\kappa = 32.8$ rad^{-2}.

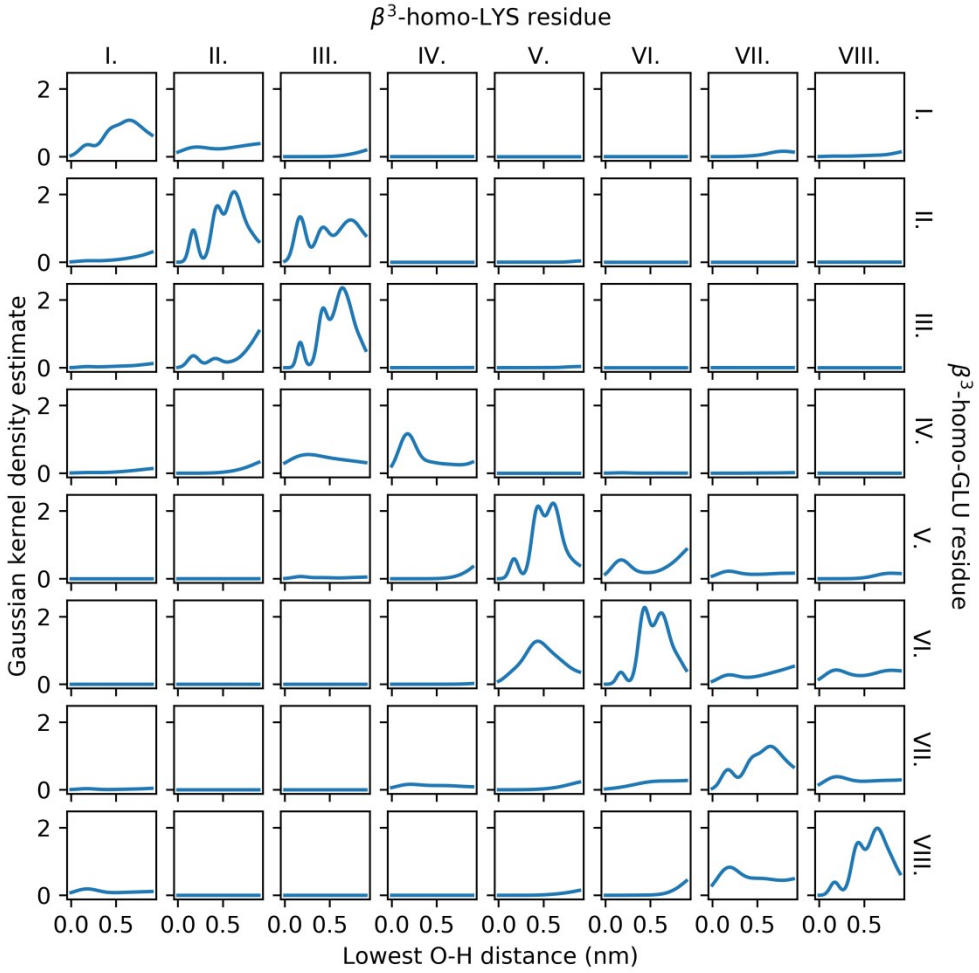

Figure S19. O-H distance distribution of salt bridges formed by β³-homoglutamate and β³-homolysine side-chains in peptide **5**. Numbers I. – VIII. correspond to the individual peptide molecules.

		LYS residue							
		I.	II.	III.	IV.	V.	VI.	VII.	VIII.
GLU residue	I.	7.02%	9.44%	0.00%	0.00%	0.00%	0.00%	0.02%	0.38%
	II.	1.04%	10.72%	20.78%	0.00%	0.00%	0.00%	0.00%	0.00%
	III.	0.66%	5.64%	7.34%	0.00%	0.00%	0.00%	0.00%	0.00%
	IV.	0.58%	0.00%	20.20%	27.13%	0.00%	0.28%	0.00%	0.00%
	V.	0.00%	0.00%	1.36%	0.00%	7.08%	14.08%	6.28%	0.00%
	VI.	0.00%	0.00%	0.00%	0.00%	9.18%	4.20%	7.36%	12.08%
	VII.	0.80%	0.00%	0.00%	4.72%	0.00%	1.52%	10.94%	11.74%
	VIII.	5.96%	0.00%	0.00%	0.00%	0.00%	0.00%	24.24%	5.14%

Table S2. Salt-bridge/ hydrogen bond occupancies between the glutamate and lysine side chains in peptide **5**. The salt bridge was considered when the distance of the hydrogen ions in the $–NH_3^+$ - group to the oxygens in the $–COO^-$ - group was less than 0.3 nm. Numbers I. – VIII. correspond to the individual peptide molecules.

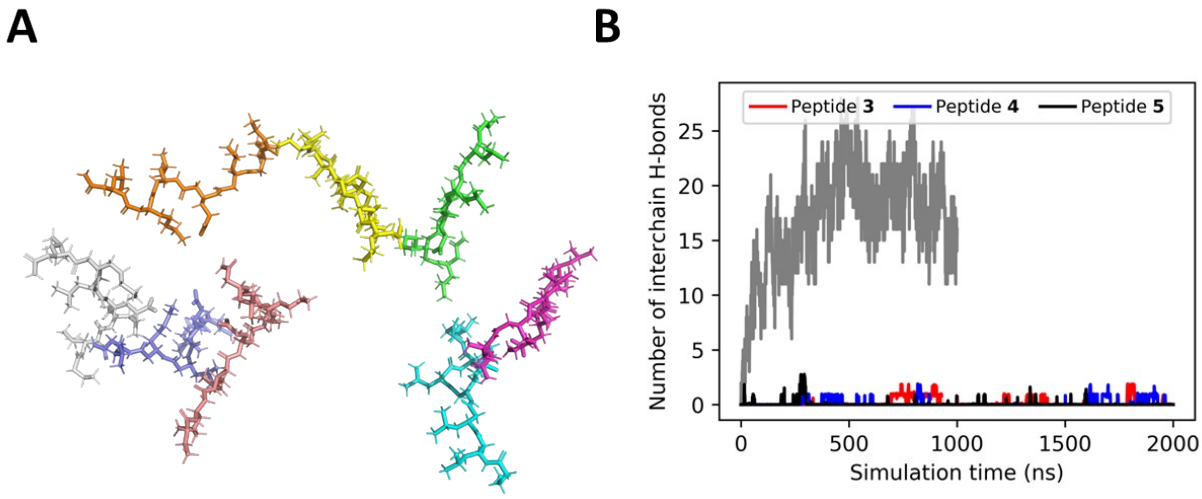

Figure S20. Structures obtained from simulation in methanol. A.) representative snapshot of the system of eight chains of peptide **5** in methanol. Colors correspond to different chains. B.) number of interchain hydrogen bonds in peptide **3** (red), **4** (blue) and **5** (black) in methanol. For comparison peptide **5** (grey) in water is also displayed here from Figure 4 panel D.

Restraints	**k / (kJ mol^{-1} nm^{-2})**						
	STEP0	STEP1	STEP2	STEP3	STEP4	STEP5	STEP6
5 sidechain	4000	4000	2000	1000	500	200	100
5 backbone	2000	2000	1000	500	200	50	50
DOPC phosphorous atom	1000	1000	1000	400	200	40	0
DOPC dihedral	1000	1000	400	200	200	100	0
water	1000	1000	1000	1000	1000	0	0

Table S3. Applied atomic restraints during the minimization and equilibration process.

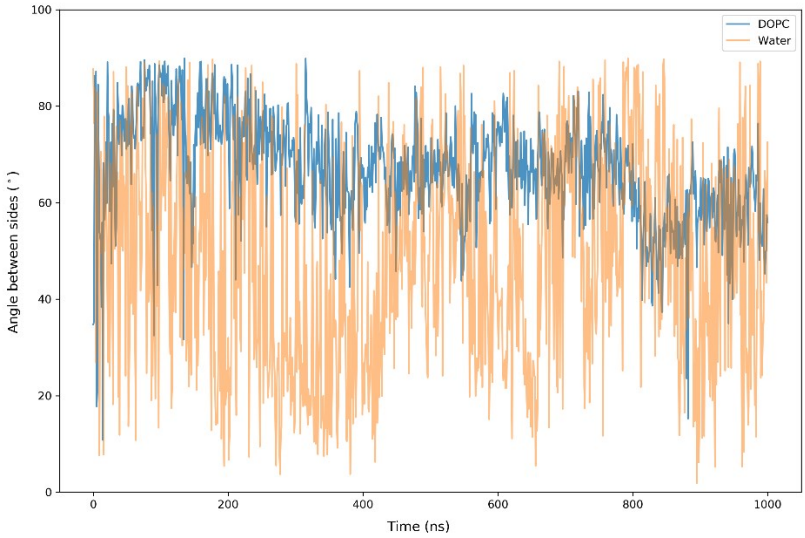

Figure S21. Relative angle between layer I. and layer II. in the two-layered octameric oligomers of peptide **5** in water and in lipid bilayer as observed in the MD simulations. The directions of the two layers are obtained as the average of the directions for each monomer present in the particular layer. The direction of one monomer was obtained by fitting a vector on the αC atoms of every residue in the selected monomer.

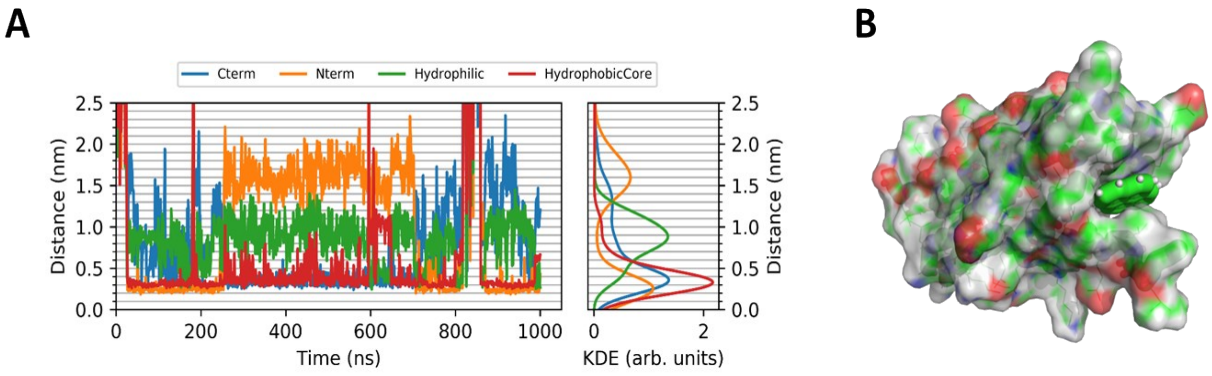

Figure S22. Average localization of pyrene molecule in octameric form of peptide **5** from MD simulation. A.) Distance of the COM of pyrene molecule from the following four atom groups: all atoms of the C-terminal leucine residues ("Cterm", blue line), non-hydrogen atoms of the N-terminal butyryl groups ("Nterm", orange line), ending atoms of the Glu and Lys side-chains ("Hydrophilic", green line) and the three outermost carbon atoms of the Leu side-chains of residues 3-5 ("HydrophobicCore", red line) (left). Gaussian kernel density estimates (0.158 nm bandwidth, determined using Scott's rule of thumb) (right). B.) Pyrene molecule localization in the octameric form of peptide **5** (Color code: carbon, *green*, nitrogen, *blue*, oxygen, *red*)

7. Differential scanning calorimetry

Sample	Pre-transition		Main transition	
	T_m (˚C)	ΔH (kJ/mol)	T_m (˚C)	ΔH (kJ/mol)
DPPC/PBS	35.4	3.82	41.58	29.1
DPPC/**3**	-	-	41.49	23.5
DPPC/**4**	-	-	41.23	24.5
DPPC/**5**	-	-	41.56	21.0

Table S4. Phase transition parameters obtained from **DPPC/"RS"** multilamellar liposomal-peptide systems.

8. Circular dichroism spectroscopy

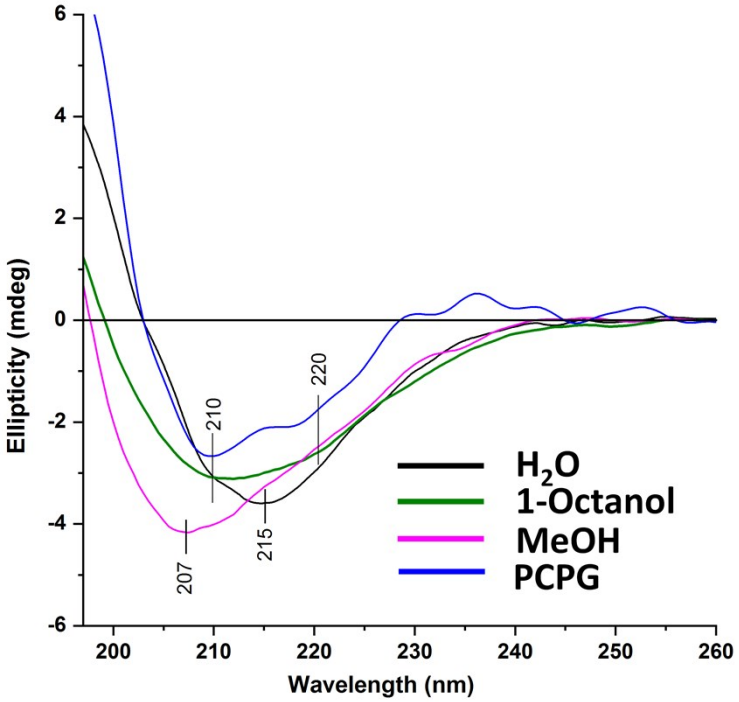

Figure S23. Far-UV CD spectra of peptide **5** in solvents with different polarity. Spectra were collected at 0.2 mM peptide concentration in water, octanol and methanol and at 0.13 mM peptide with PCPG liposomes (1.3 mM total lipid) concentration. Note that for graphical reason the spectra of PCPG are multiplied by 2.5.

References

1 A. M. Weljie, *Protein Sci.*, 2003, **12**, 228–236.
2 T. D. W. Claridge, *High-resolution NMR techniques in organic chemistry*, Elsevier, Amsterdam, 2. ed., 2009.
3 A. Wacha, T. Beke-Somfai and T. Nagy, *ChemPlusChem*, 2019, **84**, 927–941.
4 G. Bussi, D. Donadio and M. Parrinello, *J. Chem. Phys.*, 2007, **126**, 014101.
5 H. J. C. Berendsen, J. P. M. Postma, W. F. van Gunsteren, A. DiNola and J. R. Haak, *J. Chem. Phys.*, 1984, **81**, 3684–3690.
6 S. Nosé, *Mol. Phys.*, 1984, **52**, 255–268.
7 W. G. Hoover, *Phys. Rev. A*, 1985, **31**, 1695–1697.
8 S. Nosé and M. L. Klein, *Mol. Phys.*, 1983, **50**, 1055–1076.
9 M. Parrinello and A. Rahman, *J. Appl. Phys.*, 1981, **52**, 7182–7190.
10 S. Jo, J. B. Lim, J. B. Klauda and W. Im, *Biophys. J.*, 2009, **97**, 50–58.
11 E. F. Pettersen, T. D. Goddard, C. C. Huang, G. S. Couch, D. M. Greenblatt, E. C. Meng and T. E. Ferrin, *J. Comput. Chem.*, 2004, **25**, 1605–1612.
12 K. Vanommeslaeghe, E. Hatcher, C. Acharya, S. Kundu, S. Zhong, J. Shim, E. Darian, O. Guvench, P. Lopes, I. Vorobyov and A. D. Mackerell, *J. Comput. Chem.*, 2009, NA-NA.
13 W. Yu, X. He, K. Vanommeslaeghe and A. D. MacKerell, *J. Comput. Chem.*, 2012, **33**, 2451–2468.